International Journal of Advanced Robotic Systems

OPEN ACCESS ARTICLE

Heading Control for a Robotic Dolphin Based on a Self-tuning Fuzzy Strategy

Regular Paper

Zhiqiang Cao[1], Fei Shen[2]*, Chao Zhou[1], Nong Gu[3], Saeid Nahavandi[3] and De Xu[2]

1 State Key Laboratory of Management and Control for Complex Systems, Institute of Automation, Chinese Academy of Sciences, Beijing, China
2 Research Center of Precision Sensing and Control, Institute of Automation, Chinese Academy of Sciences, Beijing, China
3 Centre for Intelligent Systems Research, Deakin University, Australia
*Corresponding author(s) E-mail: fei.shen@ia.ac.cn

Received 03 October 2015; Accepted 22 January 2016

DOI: 10.5772/62289

Abstract

In this paper, a heading controller based on a self-tuning fuzzy strategy for a robotic dolphin is proposed to improve control accuracy and stability. The structure of the robotic dolphin is introduced and the turning motion is analysed. The analytic model indicates that the turning joint angle can be employed for the heading control. This non-linear model prevents the successful application of traditional model-based controllers. A fuzzy controller is proposed to realize the heading control in our work. It should be mentioned that the traditional fuzzy controller suffers from a distinguished steady-state error, due to the fact that the heading range is relatively large and the fuzzy controller's universe of discourse is fixed. To resolve this problem, a self-tuning mechanism is employed to adjust the input and output scaling factors according to the active working region in pursuit of favourable performance. Experimental results demonstrate the performance of the proposed controller in terms of steady-state error and robustness to interferences.

Keywords Robotic Dolphin, Heading Control, Turning Motion, Self-tuning Fuzzy Control

1. Introduction

In recent decades, extensive efforts have focused on researching unmanned underwater vehicles [1, 2] for marine resource exploitation, ocean exploration and rescue services. The efficient propulsion and good manoeuvrability of marine animals, such as cetaceans and fish, have motivated researchers to take advantage of these properties to create novel advanced underwater vehicles. Against this background, some bio-inspired swimming robots have been developed: robotic fish [3-6], a jellyfish- and butterfly-inspired microrobot [7], and a robotic dolphin. As one kind of cetaceans, dolphins are regarded as one of the best ocean swimmers in that the propulsive efficiency of dolphins can reach up to 0.75-0.9 and the maximum swimming speed is over 11m/s. Moreover, dolphins can also achieve excellent turning manoeuvrability and rotate their bodies with an angular speed of 450°/s with turning radii down to 11-17% of body length (BL) [8].

Attracted by these desired skills, many researchers have focused on developing dolphin-like robots. Fruitful research outcomes have been achieved in the areas of mechatronic design, hydrodynamics analysis and control schemes. Pioneering research in mechatronic design has led to several typical prototypes, including a two-joint robotic dolphin [9, 10], a four-joint pneumatic robotic dolphin [11], a five-joint robotic dolphin with a pair of two-degrees-of-freedom (2-DOF) pectoral fins, a robotic dolphin with a two-motor-driven scotch yoke mechanism [12, 13], and a multi-link robotic dolphin with 3-DOF flippers [14]. Many researchers devote themselves to the

hydrodynamics analysis of robotic dolphins, which result in improved control performance. Dogangil *et al.* presented a dynamical behaviour model using the Newton-Euler formulation [11]. Shen *et al.* developed a propulsive dynamic model based on Kane's method, which enables the speed optimization of the robotic dolphin [15]. To mimic different swimming motions of dolphins, several control schemes have been implemented. Nakashima *et al.* focused on the roll and loop-the-loop motion with PD control [10], while Wang *et al.* aimed to achieve a porpoising motion to save energy at high speed [16]. Shen *et al.* proposed a fuzzy PID controller, which allows a robotic dolphin to cruise within a given depth [17]. Moreover, two hybrid acrobatic stunts, i.e., front flip and backflip, were implemented in a robotic dolphin by Yu [18]. It should be noted that there is urgent need to maintain a consistent heading direction for a robotic dolphin, which is a prerequisite for long-time navigation. However, heading control is challenging because unavoidable waves and turbulences in open water raise unexpected disturbances. These disturbances will force robotic dolphins to deviate from their desired courses.

In this paper, a multi-link robotic dolphin with a turning joint is designed to realize the turning motion, which paves the foundation for the heading control. Based on a hydrodynamic model, the turning motion analysis is carried out, which indicates that one can employ the yaw angle of the turning joint to control the heading, while the relationship between these two variables is non-linear. Similar to robotic fish [19, 20], it is very difficult to establish a precise mathematical model, since the heading control of a robotic dolphin involves both hydrodynamics of the fluid environment and dynamics of the robot. In this case, the fuzzy controller provides an effective solution. In this paper, a self-tuning fuzzy heading controller is proposed to mitigate the non-linearity and reject the unexpected disturbances mentioned above.

The rest of this paper is organized as follows. Section 2 introduces the structure of a robotic dolphin; the turning motion is also analysed. Section 3 presents a self-tuning fuzzy heading controller. The experimental results are given in Section 4. Finally, the paper is concluded.

2. Structure of a Robotic Dolphin and Turning Motion Analysis

2.1 Structure of a Robotic Dolphin

In nature, dolphins achieve turning manoeuvre either by flexing the anterior body laterally with a special turning unit, or flapping and rotating flippers to produce a yawing moment. Furthermore, they can simultaneously adopt these two modes to achieve a more agile and swift turning [21]. Inspired by this fact, two methods are usually employed to achieve the turning motion of a robotic dolphin. One is to design a turning mechanism between the anterior body and tail part, while the other is to adopt mechanical flippers to realize turning. Since the second method requires a sophisticated seal of pectoral fins, the former one is adopted in this paper.

An experimental robotic dolphin is given in Fig. 1, while Fig. 1(a) demonstrates the structure of the robot. Joints 1-3, which are driven by servos in the rear part of the robotic dolphin, are used to provide the propelling force. A turning joint located in the middle of the robot is designed to achieve the turning motion. The pitch motion of the robotic dolphin is implemented by a barycentre adjustment mechanism. Besides a GPS and a pressure sensor for the robotic dolphin, an inertial sensor, with its y-axis being parallel to the horizontal medial axis of the robotic dolphin, is utilized to sense the heading direction.

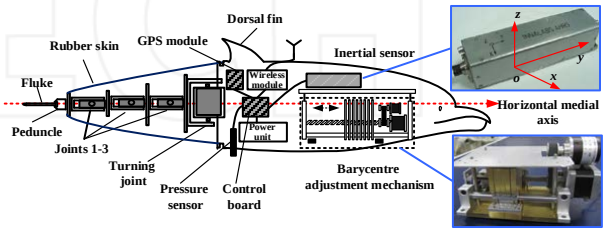

(a)

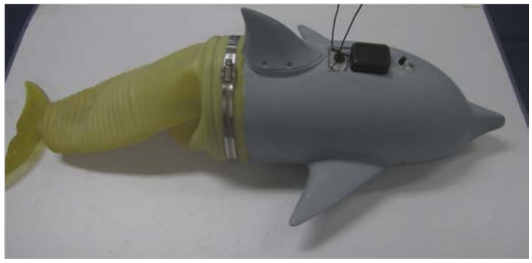

(b)

Figure 1. An experimental robotic dolphin: (a) The diagram of the robotic dolphin's structure; (b) the robotic dolphin prototype

2.2 Turning Motion Analysis

As shown in Fig. 2, a plane coordinate frame $O_1x_1z_1$ is established, where O_1 is the gravity centre of the robotic dolphin without turning motion, O_1x_1 is the horizontal medial axis of the robotic dolphin and O_1z_1 is the pitching axis perpendicular to O_1x_1 on the horizontal plane. In addition, B_2, B_3 and B_4 are labelled as the gravity centre of the whole robotic dolphin, head part and tail part, respectively, while J is the turning centre of the turning joint. We denote q_1, q_2 and q_3 with the distances between J and B_4, O_1 and B_3, and O_1 and J, respectively. When the robotic dolphin is not turning, B_2 coincides with O_1. When the tail of the robotic dolphin deviates at θ around the turning joint, the coordinate of the gravity centre of the whole robotic dolphin B_2 changes to $(\Delta x, -\Delta z)$ in $O_1x_1z_1$, where Δx and Δz are expressed as follows:

$$\Delta x = -\frac{m_t(q_3 + q_1\cos\theta) - m_h q_2}{m_h + m_t} \tag{1}$$

$$\Delta z = \frac{m_t q_1 \sin\theta}{m_h + m_t} \tag{2}$$

where m_h is the mass of the robotic dolphin's head part and m_t is the mass of the robotic dolphin's tail part, which is from the turning joint to the fluke.

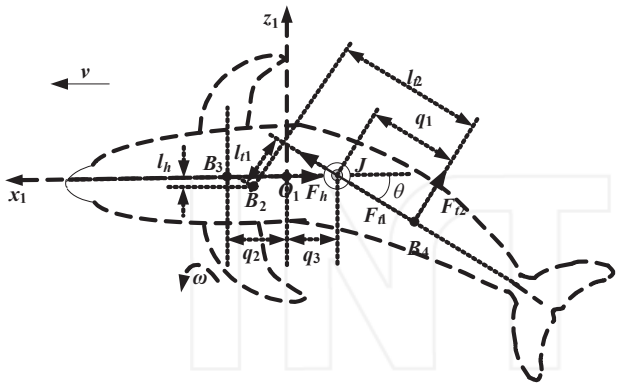

Figure 2. Turning motion analysis of the robotic dolphin

When the robotic dolphin turns with a swimming velocity $v(t)$, it can be regarded as consisting of two rigid bodies, which are head part and tail part, respectively. In the process of turning, the head of the robotic dolphin is mainly imposed by a frontal section resistance denoted as F_h, while the forces acting on the tail mainly consist of tail fin propulsion F_{t1} and lateral section resistance F_{t2}. The frontal section resistance F_h and the tail lateral section resistance F_{t2} can be calculated on the basis of the resistance model [8]:

$$F_h = 0.5\rho C_h A_h v^2(t) \tag{3}$$

$$F_{t2} = 0.5\rho C_{t2} A_{t2} (v(t)\sin\theta)^2 \tag{4}$$

where ρ is the density of water. C_h and A_h are the frontal section resistance coefficient and frontal section area of the dolphin head, respectively. A_{t2} is the lateral section area of the dolphin tail. C_{t2} is the lateral section resistance coefficient related to the configuration of the tail. According to [8], C_{t2} can be approximated as a constant based on the resistance model. The tail fin's force model has been analysed in detail in previous work [15]. The hydrodynamic force is derived by modelling the tail fin as a finite span hydrofoil or a flat plate based on lifting-line theory and resistance model, respectively, according to different ranges of its attack angle. With a certain tail flapping frequency and amplitude, F_{t1} can be expressed as a function of v:

$$F_{t1} = f(v) = \begin{cases} 0.5\rho A_{t1}(v(t)\cos\theta)^2 (C_L + C_{D,i} + C_{D,x}) & \alpha \in (-\alpha_{stall}, \alpha_{stall}) \\ 0.5\rho A_{t1}(v(t)\cos\theta)^2 C_{t1} & \alpha \notin (-\alpha_{stall}, \alpha_{stall}) \end{cases} \tag{5}$$

where A_{t1} is the tail fin area of the robotic dolphin. C_L, $C_{D,i}$, $C_{D,x}$ and C_{t1} are the coefficients of lift, induced drag, profile drag and section drag, respectively. α is the attack angle of the tail fin and α_{stall} is the stalling angle of attack. The yawing moment M formed by the above forces is:

$$M = F_h l_h + F_{t1} l_{t1} + F_{t2} l_{t2} \tag{6}$$

where l_h, l_{t1} and l_{t2} are arms of F_h, F_{t1} and F_{t2}, respectively, and:

$$l_h = \Delta z \tag{7}$$

$$\begin{aligned} l_{t1} &= \frac{\Delta z}{\cos\theta} + (\Delta x - \Delta z \tan\theta + q_3)\sin\theta = \\ &= \frac{m_h(q_2 + q_3)}{m_h + m_t}\sin\theta \end{aligned} \tag{8}$$

$$\begin{aligned} l_{t2} &= q_1 + (\Delta x - \Delta z \tan\theta + q_3)\cos\theta = \\ &= \frac{m_h}{m_h + m_t}[q_1 + (q_2 + q_3)\cos\theta] \end{aligned} \tag{9}$$

On the basis of the law of rotation, one may get:

$$M = I\dot{\omega} \tag{10}$$

where I is the moment of inertia of the yawing axis and $\dot{\omega}$ is the yawing angular accelerator of the robotic dolphin. The above equation can be further written as follows:

$$\dot{\omega} = c_4\{c_1 v^2(t) + c_2 f(v) + c_3 v^2(t)[q_1 + (q_2 + q_3)\cos\theta]\sin\theta\}\sin\theta \tag{11}$$

where c_1, c_2, c_3 and c_4 are constants, and $c_1 = 0.5\rho C_h A_h m_t q_1$, $c_2 = m_h(q_2 + q_3)$, $c_3 = 0.5\rho C_{t2} A_{t2} m_h$, $c_4 = 1/[I(m_h + m_t)]$.

Hence, the real-time heading angle of the robotic dolphin $\varphi(t)$ is given as:

$$\begin{aligned}\varphi(t) &= \int_0^t (\int_0^t \dot{\omega}(t)dt + \omega_0)dt + \varphi_0 \\ &= \int_0^t (\int_0^t c_4\{c_1 v^2(t) + c_2 f(v) + c_3 v^2(t)[q_1 + (q_2 + q_3)\cos\theta]\sin\theta\}\sin\theta dt + \omega_0)dt + \varphi_0\end{aligned} \tag{12}$$

where ω_0 and φ_0 are the initial yawing angular rate and initial yaw angle of the robotic dolphin, respectively.

One can see from (12) that the robotic dolphin's heading $\varphi(t)$ can be controlled by adjusting the turning joint angle $\theta(t)$ with a swimming velocity $v(t)$. Moreover, the relationship between $\varphi(t)$ and $\theta(t)$ is non-linear. Given the non-linear relationship between the control variable (turning joint angle) and the target variable (the heading of robotic dolphin), as well as the complexity of hydrodynamics, the traditional model-based controllers are not feasible anymore. Since the fuzzy logic control does not require an accurate model, a fuzzy-based approach is presented to solve the heading control problem.

3. Heading Control of a Robotic Dolphin Based on a Self-tuning Fuzzy Strategy

3.1 Heading Control System

Fig. 3 illustrates the developed control system. This system mainly includes a fuzzy controller, a self-tuning mechanism, a servo and an inertial sensor, wherein the sensor is employed to measure the heading φ of the robotic dolphin in real time. The input of the self-tuning fuzzy controller is the heading error, while its output is fed into the servo to change the turning angle θ of the turning joint. To mitigate the interference in the environment, the proposed fuzzy controller is designed to produce a fast response and compensate the big error. Nevertheless, when the input is small, the working region is confined to the region of ZE fuzzy set, which causes the controller output to remain almost unchanged. Thus, the steady-state error is produced as the heading range is relatively large and the fuzzy controller's universe of discourse is fixed. One solution is to further refine the fuzzy membership functions to improve the sensitivity of the controller, but it will inevitably increase the complexity of the fuzzy controller. Since the input and output scaling factors are respectively used to transfer the controller input and output into the universe of discourse and the actual control variable range, a self-tuning mechanism for tuning the input and output scaling factors is designed to improve the sensitivity of the controller, as well as the steady-state accuracy of the system.

3.2 Design of the Self-tuning Controller

The inputs of the fuzzy controller are heading error $e(k)$ and differential error $ec(k)$, which are defined as $e(k)=\varphi^*(k)-\varphi(k)$ and $ec(k)=e(k)-e(k-1)$, respectively. $\varphi^*(k)$ is the target heading, $\varphi(k)$ is the feedback heading and k is the sampling index. It should be noted that the output of the inertial sensor $\varphi_c(k)$ is in the range of 0°~360°. If the value of $\varphi(k)$ is directly taken from $\varphi_c(k)$ and it switches between the first quadrant 0°~90° and the fourth quadrant 270°~360°, the error $e(k)$ will experience a sudden change. Thus, to ensure $e(k)$ continuous change in the interval (-180°~180°), $\varphi(k)$ should be given as

$$\varphi(k) = \begin{cases} \varphi_c(k) + 360 & \varphi_c(k) \in (0, \varphi^*(k) - 180) \cap \varphi^*(k) \in (180, 360] \\ \varphi_c(k) - 360 & \varphi_c(k) \in (180 + \varphi^*(k), 360) \cap \varphi^*(k) \in [0, 180) \\ \varphi_c(k) & \text{others} \end{cases} \tag{13}$$

3.2.1 Membership Function Design

Triangular membership functions with a 50% overlap on neighbours are used for e, ec and u, as shown in Fig. 4. For the input e and ec as well as the output u, labelled as E, EC and U, respectively, seven linguistic values are adopted as follows:

$$\begin{aligned} \mathrm{E} &= \{\mathrm{NB},\ \mathrm{NM},\ \mathrm{NS},\ \mathrm{ZE},\ \mathrm{PS},\ \mathrm{PM},\ \mathrm{PB}\} \\ \mathrm{EC} &= \{\mathrm{NB},\ \mathrm{NM},\ \mathrm{NS},\ \mathrm{ZE},\ \mathrm{PS},\ \mathrm{PM},\ \mathrm{PB}\} \\ \mathrm{U} &= \{\mathrm{NB},\ \mathrm{NM},\ \mathrm{NS},\ \mathrm{ZE},\ \mathrm{PS},\ \mathrm{PM},\ \mathrm{PB}\} \end{aligned} \tag{14}$$

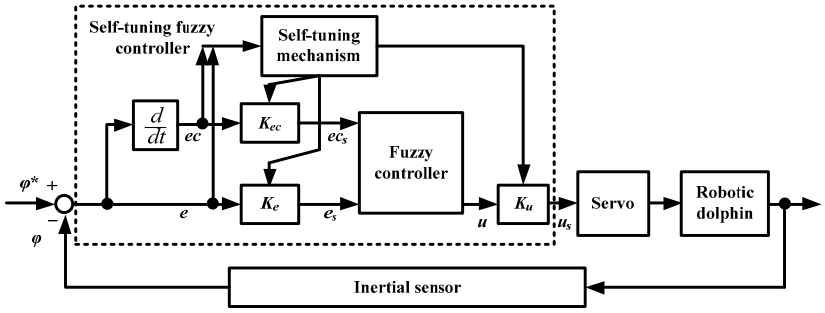

Figure 3. The heading controller of a robotic dolphin based on a self-tuning fuzzy strategy

where NB, NM, NS, ZE, PS, PM and PB are linguistic values, which denote negative large, negative middle, negative small, zero, positive small, positive middle and positive large, respectively.

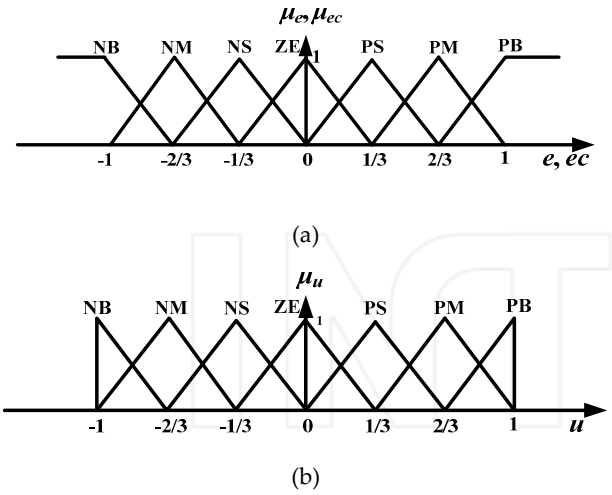

Figure 4. (a) Membership functions for *e* and *ec*; (b) membership function for *u*

3.2.2 Fuzzy Rule Base Design

The rule base reflecting the intelligence of the fuzzy control is responsible for specifying the actions that shall be taken under different situations. Taking advantage of the experimental experience of the robotic dolphin's turning motion, the rule base is obtained as shown in Table 1. Each rule in the rule base has the IF-THEN form. Since position control type is adopted for the fuzzy control, the rule base is established by obeying the following principles:

i. When the heading error is positive (negative) large and the error change is positive (negative) large, it indicates that the heading is deviated largely from the target heading and the heading error is rapidly increasing. Thus, the control variable U should be positive (negative) large to eliminate the error as soon as possible.

ii. When the heading error is positive (negative) small or zero and the error change is negative (positive) large, it indicates that, although the current heading is close to the target, the heading error still has the increasing trend because it is reduced excessively. Thus, the control variable U should be negative (positive) small or negative (positive) large, respectively, to prevent overshoot.

3.2.3 Defuzzification

Here, the commonly used centre of gravity defuzzification is adopted:

$$u = \frac{\sum_{i=1}^{m} b_h \mu_i(E_j, EC_k, U_h, e, ec)}{\sum_{i=1}^{m} \mu_i(E_j, EC_k, U_h, e, ec)} \tag{15}$$

where u is the defuzzification output of the fuzzy controller, m is the number of the enabled fuzzy rules in the rule base, b_h is membership function centre of the fuzzy output language variable, and $\mu_i(E_j, EC_k, U_h, e, ec)$ is the membership value of the ith fuzzy rule obtained according to fuzzy reasoning, which is calculated by:

$$\mu_i(E_j, EC_k, U_h, e, ec) = \mu_{E_j}(e) \wedge \mu_{EC_k}(ec) \wedge \mu_{U_h}(u) \tag{16}$$

3.2.4 Self-tuning Mechanism

Since the target heading is in a large range (0°~360°), the fuzzy controller input, including heading error and error change, will vary over a large range. For the regular fuzzy controller, the input and output scaling factors are set according to the entire range and remain unchanged in the whole process. When the heading error is large, the fuzzy controller is able to respond quickly to reduce the error. When the heading error is small, however, the working region is confined to the region of the ZE fuzzy set, which will cause a steady-state error. In this case, a self-tuning mechanism is designed to tune the input scaling factors to expand the working region for improving the input resolution [22]. Accordingly, the output of our controller is changed by tuning the output scaling factor to improve the performance of the controller. Based on these ideas, the self-tuning mechanism adopts the piecewise way to realize the

U		E						
		NB	***NM***	***NS***	***ZE***	***PS***	***PM***	***PB***
EC	***NB***	NB	NB	NM	NB	NS	PS	PM
	NM	NB	NB	NM	NM	NS	PM	PB
	NS	NB	NM	NS	NS	ZE	PM	PB
	ZE	NB	NM	NS	ZE	PS	PM	PB
	PS	NB	NM	ZE	PS	PS	PM	PB
	PM	NB	NM	PS	PM	PM	PB	PB
	PB	NM	NS	PS	PB	PM	PB	PB

Table 1. Rule base of fuzzy controller

tuning according to the range of the heading error. When the heading error is in a large range, fixed scaling factors are adopted. When the heading error is in a small area, variable scaling factors are designed as follows:

$$K_e = \begin{cases} \dfrac{1}{e_{\max}} & |e| > e_{th} \\ \dfrac{1}{e_{\max t}} & |e| \le e_{th} \end{cases}, \quad K_{ec} = \begin{cases} \dfrac{1}{ec_{\max}} & |e| > e_{th} \\ \dfrac{1}{ec_{\max t}} & |e| \le e_{th} \end{cases}, \quad K_u = \begin{cases} u_{\max} & |e| > e_{th} \\ \beta \dfrac{e_{\max t} u_{\max}}{e_{\max}} & |e| \le e_{th} \end{cases}, \tag{17}$$

where K_e, K_{ec} and K_u are scaling factors of heading error e, error change ec and output u, respectively. e_{th} is the threshold of the heading error. $e_{\max}$, $ec_{\max}$ and $u_{\max}$ are respectively the maximum value of heading error, error change and the output. $e_{\max t}$ and $ec_{\max t}$ are the maximum value of heading error and error change in the self-tuning period T. β is the regulating factor for amplifying the output of the controller appropriately.

Using the above scaling factors, the regularized heading error, error change and output, defined in [-1, 1], can be obtained as:

$$e_s = K_e e, \ ec_s = K_{ec} ec, \ u_s = K_u u \tag{18}$$

4. Experimental Results

To verify the rationality of the proposed controller, a series of experiments was conducted in a lake including comparison experiment, anti-interference experiment and heading switching experiment. The parameters of input and output scaling factors and other parameters of the controller are given as: $e_{\max}$=90, $ec_{\max}$=40, $u_{\max}$=60, e_{th}=5, T=1.8s and β=2.5. In addition, to maintain the propulsion, the robotic dolphin oscillates its tail at a frequency of 2.3Hz and the control period of the system was 0.62s. The static accuracy and dynamic accuracy of the adopted inertial sensor are 0.3° and 0.7°, respectively.

4.1 Heading Control Experiment Based on a Self-tuning Fuzzy Controller

Fig. 5 depicts the experimental results of heading control with an initial heading of 273° and a target heading of 140°, and the curves of heading and heading error, K_e, K_{ec} and K_u are demonstrated.

From the heading curve, one can see that the controller responds quickly to reduce the heading error, and the heading approaches the target direction after 7s. The curves of heading error, K_e, K_{ec} and K_u, are given after convergence. As shown in the curves of K_e, K_{ec} and K_u, the input and output scaling factors are adjusted in each self-tuning period. The heading error curve proves that our controller achieves an effective heading control.

4.2 Contrast Experiment with Regular Fuzzy Control

To further validate the performance of the self-tuning fuzzy controller, the comparative experiment with a regular

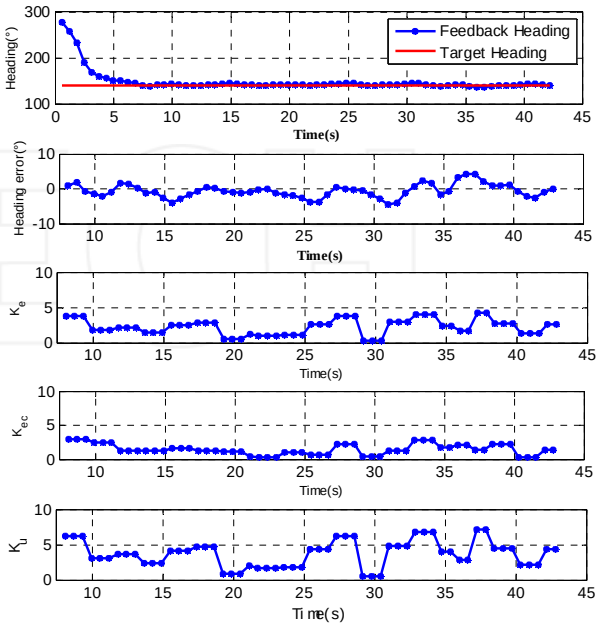

Figure 5. The heading control experiment for a robotic dolphin based on a self-tuning fuzzy controller

fuzzy controller was carried out. Since the input and output scaling factors of a regular fuzzy controller is fixed throughout the control process, the self-tuning fuzzy controller becomes a regular fuzzy controller when the threshold of the heading error e_{th} is set to 0.

Fig. 6 shows the contrast experimental results with the target heading angle of 150°. One can see that both the regular fuzzy controller and fuzzy self-tuning controller can quickly eliminate large errors. However, a distinguished steady-state error within a range of 3° to 8° exists in the regular fuzzy controller (see Fig. 6(a)). This steady-state error cannot be eliminated due to fixed scaling factors of the controller. In contrast, as shown in Fig. 6(b), a better convergence performance can be obtained by our controller due to the self-tuning mechanism.

4.3 Anti-interference Experiment

Fig. 7 shows the result of an anti-interference experiment with the target heading of 321°. At first, the heading of the robotic dolphin changes rapidly from an initial heading of 144° to the target heading. After 10s, the heading begins to maintain itself in the vicinity of the target heading. A man-made interference is then suddenly imposed on the robotic dolphin, which results in a deviation of about 50° from the

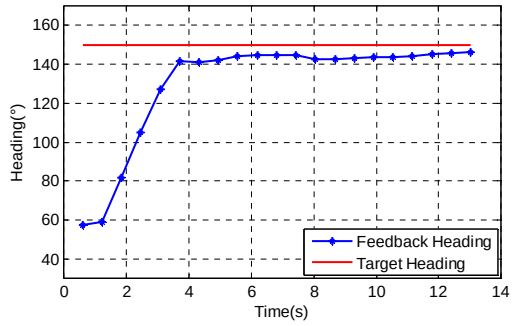

(a) Regular fuzzy control

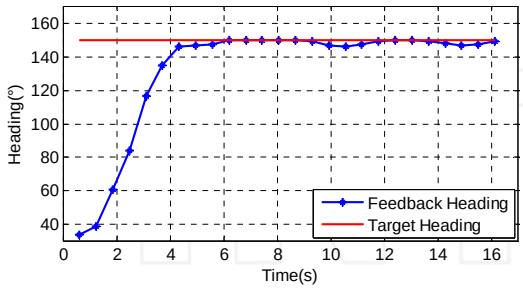

(b) Self-tuning fuzzy control

Figure 6. Results of comparison with regular fuzzy control

target heading. After that, the heading of the robotic dolphin is re-stabilized around the target heading, which indicates the robustness of the proposed self-tuning fuzzy controller.

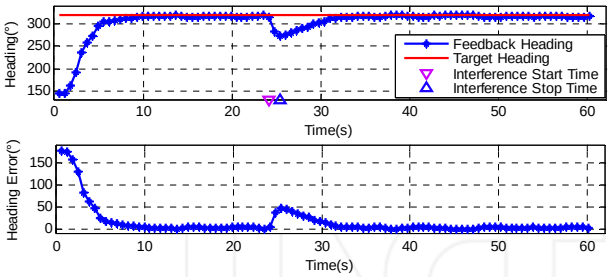

Figure 7. Results of an anti-interference experiment

4.4 Heading Switching Experiment

The experimental result of heading switching is provided in Fig. 8. In the initial stage, the robotic dolphin swims with a target heading of 330°. After the target heading is reset to 150°, the robotic dolphin responds quickly and steady swimming with the new target heading is achieved after 10s.

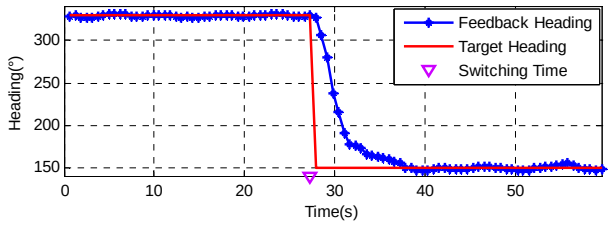

Figure 8. Result of a heading switching experiment

5. Conclusion

In this paper, we have developed a fuzzy control method to achieve a robust heading control for a multilink robotic dolphin. The turning motion of a robotic dolphin is analysed. Considering the severe non-linearity in heading control and disturbances due to water waves and turbulences, a self-tuning fuzzy controller is presented to improve the rapid response ability and the steady-state accuracy of the control system. The effectiveness of the proposed method is verified by experiments. In the future, we will conduct hydrodynamics validation based on the deduced turning motion analysis model.

6. Acknowledgements

This work was supported in part by the National Natural Science Foundation of China, under Grants 61421004 and 61473295, and in part by the Beijing Natural Science Foundation, under Grant 4152054. Fei Shen is the corresponding author.

7. References

[1] Sun B, Zhu DQ, Yang SX: A bio-inspired cascaded approach for three-dimensional tracking control of unmanned underwater vehicles. Int. J. Robot. Autom. 2014;29(4):349-358.

[2] Zhu DQ, Liu J, Yang SX: Particle swarm optimization approach to thruster fault-tolerant control of unmanned underwater vehicles. Int. J. Robot. Autom. 2011;26(3):282-287.

[3] Low KH: Design, development and locomotion control of bio-fish robot with undulating anal fins. Int. J. Rob. and Auto. 2007;22(1):88-99.

[4] Zhou C, Cao ZQ, Wang S, Tan M: The design, modelling and implementation of a miniature biomimetic robotic fish. Int. J. Robot. Autom. 2010;25(3):210-216.

[5] Siahmansouri M, Ghanbari A, Fakhrabadi MMS: Design, implementation and control of a fish robot with undulating fins. Int. J. Adv. Robot. Syst. 2011;8(5):61-69.

[6] Chowdhury AR, Panda SK: Brain-map based carangiform swimming behaviour modeling and control in a robotic fish underwater vehicle. Int. J. Adv. Robot. Syst. 2015;doi:10.5772/60085.

[7] Shi LW, Guo SX, Asaka K: A novel jellyfish- and butterfly-inspired underwater microrobot with pectoral fins. Int. J. Robot. Autom. 2012;27(3): 276-286.

[8] Fish FE, Rohr JJ: Review of dolphin hydrodynamics and swimming performance. San Diego: United State Navy, Technical Report 1801, 1999.

[9] Nakashima M, Ono K: Development of a two-joint dolphin robot. In Neurotechnology for Biomimetic

Robots. J Ayers, JL Davis and A Rudolph, Eds. Cambridge, MA: MIT Press, 2002;309-324.

[10] Nakashima M, Tsubaki T, Ono K: Three-dimensional movement in water of the dolphin robot-Control between two positions by roll and pitch combination. J. Robot. Mechatron. 2006;18(3):347-355.

[11] Dogangil G, Ozcicek E, Kuzucu A: Modeling, simulation, and development of a robotic dolphin prototype. In Proc. IEEE Int. Conf. Mechatron. Autom. Canada, 2005;952-957.

[12] Yu J, Hu Y, Fan R, Wang L, Huo J: Mechanical design and motion control of a biomimetic robotic dolphin. Advan. Robot. 2007;21(3-4):499-513.

[13] Yu J, Hu Y, Huo J, Wang L: Dolphin-like propulsive mechanism based on an adjustable Scotch yoke. Mech. Mach. Theory. 2009;44(3):603-614.

[14] Shen F, Wei C, Cao Z, Xu D, Yu J, Zhou C: Implementation of a multi-link robotic dolphin with two 3-DOF flippers. J. Comput. Inf. Syst. 2011;7(7): 2601-2607.

[15] Shen F, Cao Z, Xu D, Zhou C: A dynamic model of robotic dolphin based on Kane method and its speed optimization method. Acta Automatica Sinica. 2012;38(8):1247-1256.

[16] Wang Y, Yu J, Zhang J: Modeling and simulation of porpoising for a multilink dolphin robot. In Proc. IEEE Int. Conf. Robot. Biomim. Thailand, 2011;2131-2136.

[17] Shen F, Cao Z, Zhou C, Xu D, Gu N: Depth control for robotic dolphin based on fuzzy PID control. Int. J. Offshore Polar Eng. vol. 23, no. 3, 2013;166-171.

[18] Yu J, Su Z, Wang M, Tan M, Zhang J: Control of yaw and pitch maneuvers of a multilink dolphin robot. IEEE Trans. Robotics. 2012;28(2):318-329.

[19] Yu J, Tan M, Wang S, Chen E: Development of a biomimetic robotic fish and its control algorithm. IEEE Trans. Systems, Man Cybernetics. 2004; 34(4): 1798-1810.

[20] Yu J, Liu L, Wang L, Tan M, Xu D: Turning control of a multilink biomimetic robotic fish. IEEE Trans. Robotics. 2008; 24(1):201-206.

[21] Yu J, Li YF, Wang M, Tan M: Turning analysis and its implementation of link-based dolphin-like robots. In Proc. IEEE Int. Conf. Autom. Logist. Qingdao, 2008;1172-1177.

[22] Fang Z, Xu D, Tan M: A vision-based self-tuning fuzzy controller for fillet weld seam tracking. IEEE/ASME Trans. Mechatron. 2011;16(3):540-550.